5th Conference on Production Systems and Logistics

# Investigation Of Laser-Based Drying Of Electrodes For Lithium-Ion-Battery Production Using Vertical-Cavity Surface-Emitting Lasers (VCSEL)

Daniel Neb[1], Sebastian Wolf[1], Benedict Ingendoh[1], Simon Klein[2], Benjamin Dorn[1], Heiner Heimes[1], Achim Kampker[1]

[1]*Chair of Production Engineering of E-Mobility Components PEM, RWTH Aachen University, Aachen, Germany*
[2]*Faculty of Mechanical Engineering, RWTH Aachen University, Aachen, Germany*

**Abstract**

Demand for lithium-ion batteries is expected to increase significantly within the upcoming decade. This trend is already evident today. Accordingly, an increasing number of new production lines as well as extensions of existing production lines can be observed. To reduce global $CO_2$ emissions and maintain competitiveness, the development of new, more efficient production technologies is essential. At the same time, innovative production methods can make a decisive contribution to significantly improve the quality and performance of lithium-ion batteries.
Currently, the convection drying technology marks the state of the art in drying the wet-coated electrode foils. Accounting for approximately one quarter of the total energy consumption in battery production, this technology represents one of the most cost-intensive process steps along the value chain. A promising approach to increase quality and efficiency of electrode drying is the use of vertical-cavity surface-emitting lasers (VCSEL). In addition to the improved controllability compared to conventional drying processes, these also offer the advantage of a direct energy contribution that is tailored to the material. Furthermore, the exceptionally high-power density enables a reduction in machine footprint while simultaneously increasing production throughput.
In this study, the general experimental setup for vertical drying of electrodes using VCSEL technology is described. Furthermore, the main results are presented and discussed in order to derive subsequent conclusions for further improvements in quality and energy efficiency in the drying process of electrodes for lithium-ion batteries.

**Keywords**

Lithium-Ion Batteries; Battery Production; Electrode Manufacturing; Laser Drying; VCSEL

## 1. Introduction

Since the beginning of the early 1990s, lithium-ion batteries have experienced a continuous increase in importance and have become an indispensable part of our everyday lives [1]. Their field of application predominantly ranges from the consumer sector up to the electromobility segment [2]. Due to the worldwide introduction of new regulations to increase sustainable mobility, the automotive sector is undergoing far-reaching transformations, with particular focus in the rapid development of the vehicle electrification [3, 4]. Accordingly, in 2022, the EU member states and the European Parliament reached an agreement that only climate-neutral vehicles shall be permitted by 2035 [5]. The current profound change in the automotive industry illustrates the increasing importance of electrochemical storage systems [6]. As a result of this trend,

DOI: https://doi.org/10.15488/15239
ISSN: 2701-6277

global demand is expected to increase between 2 and 4 TWh by 2030 [7].
However, the further development of the underlying production processes of lithium-ion batteries still faces many hurdles and is a key challenge for the industry [6]. One of the currently greatest challenges represents the reduction of the energy required in the production process. Together with the solvent recovery, the coating and drying of the anode as well as cathode foils present one of the most cost-intensive production steps within the value chain of lithium-ion batteries [8, 9, 10]. According to DEGEN et al., about 27% of the total energy consumption is attributed to this process step [10]. Furthermore, LIU et al. quantifies the share of energy required for drying in the total consumption at 46.84% [11]. Currently, the convection drying method shown in Figure 1, presents the most commonly used method for drying the electrodes. Disadvantages of this drying method lie in the high energy and installation space requirements.

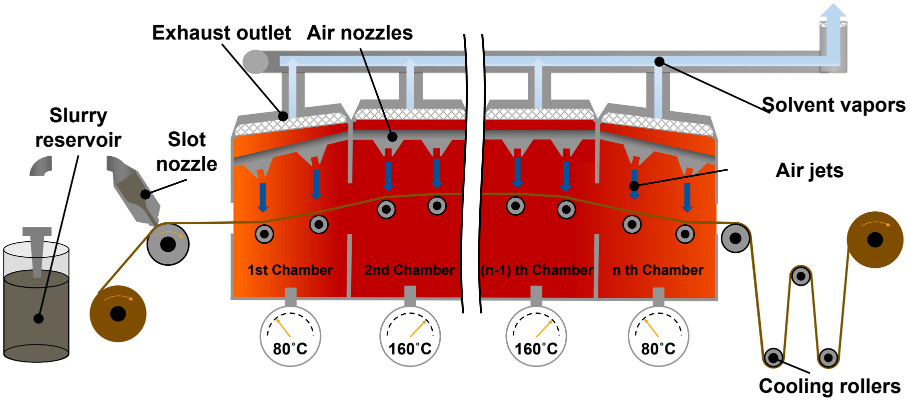


Figure 1: Coupled coating and convection drying machine of electrodes for lithium-ion battery cells

Typical production speeds of the convection drying method are in the range of 25 to 80 m/min with total furnace lengths of up to 100 meters due to the high dwell time required [8, 12]. Due to the substantial dryer length, these plants are often subject to very high investment costs [12]. Compared to alternative drying methods, the convection drying method is also characterized by relatively low energy efficiency and thus also represents a burden on the environment [13]. A further disadvantage of this drying technology lies in its poor controllability as well the limited responsiveness for changing production parameters.

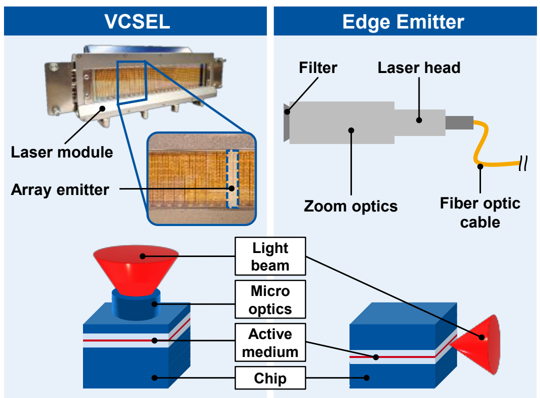


Figure 2: Comparison of VCSELs and edge emitters

A solution to this problem could be the use of lasers for drying the electrodes. This technology is characterized by high dynamic in the adjustment and control of the energy distribution on the wet coated electrode foils [14]. Furthermore, the use of laser-based drying technologies enables a reduction in energy consumption of over 50%, while at the same time increasing product quality and greatly reducing the system footprint [12, 15, 16, 17]. Figure 2 shows the two most common emitter types currently used for drying electrodes. VCSEL (vertical-cavity surface-emitting laser) are characterized by emitting their radiation perpendicular to the chip surface [18]. In contrast, the edge emitters of the diode lasers emit their radiation laterally to the chip plane [19]. The application of diode lasers for electrode drying has been extensively discussed by WOLF et al. [17, 20]. The following investigation focuses only on the use of VCSELs as an alternative technology for drying electrodes of lithium-ion batteries. According to GRONENBORN et al., VCSELs are largely scalable in power, have outstanding reliability, and offer a robust and economical solution, which makes an investigation of their application potential particularly interesting [21].

## 2. Experimental Setup

Figure 3 shows the schematic structure of the combined coating and VCSEL drying system used during the investigation. In order to reduce the risk of contamination during the manufacturing process, the machine is subdivided into individual chambers ("mini environments"). To further reduce the risk of product reactions with the surrounding process environment, each of the chambers can be operated partially or completely inerted. The test results shown in this experimental study were generated entirely under the exclusion of an inert gas atmosphere.

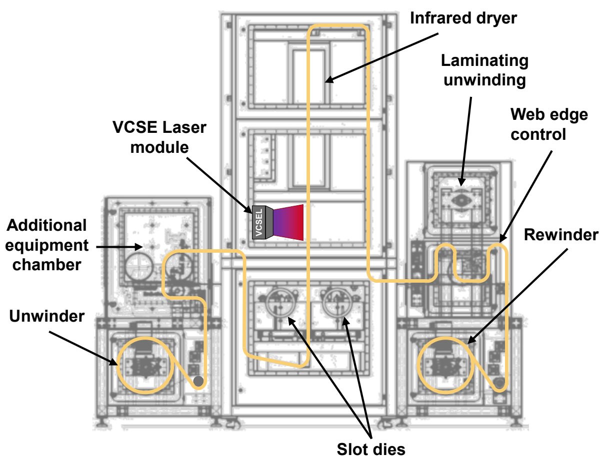


Figure 3: Schematic setup of the vertical coating line

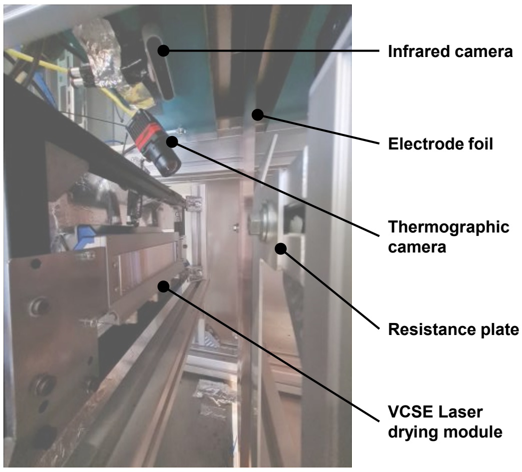


Figure 4: Setup of the VCSEL drying module inside the machine

The process starts by unwinding the foil and passing it through a chamber for additional equipment. The purpose of this second chamber is, for instance, the cleaning and activation of the film. However, no additional equipment was put into operation within the later described experiments. In the next chamber, the carrier foil is guided vertically between two opposing slot nozzles. This allows the simultaneous coating of the carrier foil on both sides without contact. Within this test series, the electrode slurries were coated centrally onto a 250 mm wide and 10 µm thick copper collector foil with a coating width of 125 mm.

Table 1 shows the composition of the three different anode slurries used during the evaluation. The utilization of different mixtures is due to the fact that the main component graphite was tested of two different material suppliers. In addition to the graphite powder, carboxy-methyl celluloses (CMC) as well as conductive carbon black are also added as further solid components to the slurry formulations.

Table 1: Composition of tested anode mixtures

| Mixture no. | 1 | 2 | 3 |
|---|---|---|---|
| Components of the mixture | Mass percentage [$wt_{solid}$ %] | | |
| Graphite | 42.3 | 38.1 | 55.4 |
| SBR | 3.4 | 3.4 | 4.4 |
| CMC | 0.9 | 0.9 | 1.2 |
| Conductive carbon black | 0.4 | 0.4 | 0.6 |
| Solvent | 53 | 57.2 | 38.4 |

For the production of the slurries, the solid and liquid components of the mixtures were homogenized by an intensive mixer. In this process, the solid components are first dry-mixed followed by the continuous addition of the solvent. The liquid components include deionized water as well as a 40 wt.% styrene butadiene rubber solution (SBR).

The coating chamber is followed by the vertical drying chamber wherein the VCSEL module is integrated. The general setup of the VCSEL drying module inside the machine is shown in Figure 4. Besides the laser drying module, the setup consists of two infrared cameras, one thermal imaging camera, an additional solvent suction system, as well as a resistance plate which cools and guides the collector foil during the laser drying process. Since only one VCSEL module was provided during the test series, only the production of single-sided coated electrodes is investigated within this study.

In addition to Figure 4, Figure 5 shows the structure of the sole VCSEL drying system. Apart from the required laser protection devices, the system also consists of the driver unit, an external cooling unit with two independent cooling circuits as well as additional connections for the energy, gas and data supply. According to PRUIJMBOOM et al. the module is specifically designed for the integration into technical equipment or machines for industrial thermal and photonic processing applications, such as drying [22]. Furthermore, the system is able to emit its energy in the form of infrared radiation at a wavelength of 980 nm.

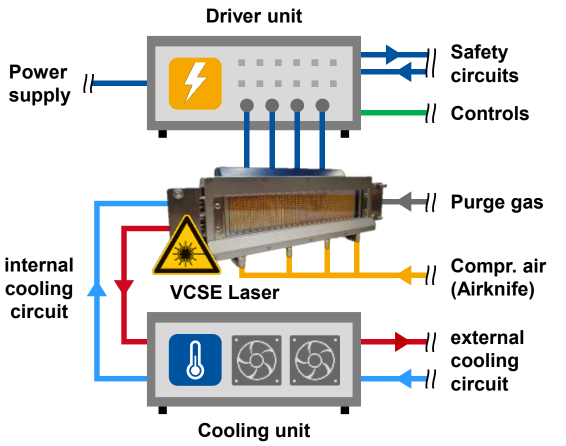


Figure 5: Structure of the sole VCSEL drying system

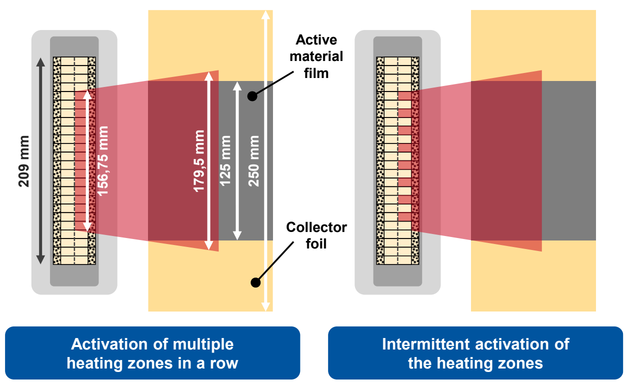


Figure 6: Independent activation of the heating zones

In total, the VCSEL module consists of 48 heating zones, which are divided into 24 VCSEL array emitters, each containing two heating zones. A heating zone consists of 28 VCSEL array chips connected in series, which measure 1.8 x 2.0 mm and contain 2205 individual VCSEL diodes [22]. This results in a rectangular emitter area of 209 x 40 mm from which the radiation is emitted. Each individual heating zone has a maximum output power of 200 W, so that a total power of up to 9.6 kW can be emitted. The area and power figures result in a maximum power density of 115 W/cm².

Figure 6 shows the experimental setup with activation of several heating zones in a row as well as intermittently activated heating zones. The output power level of the individual heating zones can be adjusted incrementally from 0 to 100%, whereby a homogeneous temperature profile can only be generated upwards the 3% level. Within the conducted experiments, the laser was operated at power levels between 5.25 and 11.5%. Following the drying process, the coated electrode foil is evenly wound up using a web edge control system.

Table 2 gives an overview of the parameter sets evaluated in this experimental study. The parameter sets were determined in the course of preliminary tests, which are not further described. The aim of the parameter study is to identify the various measurable influences on electrode quality. These influences can be divided into material related and equipment related influences, the latter being the main focus of this study. In addition to the influences of the web speed, the influences of changes in the laser power as well as the number of activated heating zones are described in the next chapter.

Table 2: Analysed parameter sets

| Parameter set no. | 1 | 2 | 3 | 4 | 5 | 6 | 7 | 8 | 9 | 10 |
|---|---|---|---|---|---|---|---|---|---|---|
| Mixture no. (acc. to table 1) | 1 | 1 | 2 | 2 | 1 | 2 | 3 | 3 | 3 | 3 |
| Web speed [m/min] | 0.8 | 0.8 | 0.8 | 1.6 | 0.8 | 1.0 | 0.8 | 0.8 | 0.8 | 0.8 |
| Pump capacity [%] | 20 | 20 | 20 | 20 | 20 | 30 | 30 | 40 | 30 | 30 |
| Laser power [%] | 5.25 | 5.75 | 11.5 | 11.5 | 6.25 | 11.5 | 5.75 | 5.75 | 5.6 | 5.6 |
| No. of activated heating zones [-] | 36 | 36 | 18 | 36 | 36 | 36 | 36 | 36 | 36 | 36 |
| Emitted power [W] | 378 | 414 | 414 | 828 | 450 | 828 | 414 | 414 | 403 | 403 |
| Power input per area [W/cm²] | 4.1 | 4.49 | 4.49 | 8.98 | 4.88 | 8.98 | 4.49 | 4.49 | 4.37 | 4.37 |
| Energy input per area [J/cm²] | 15.79 | 17.3 | 17.3 | 17.3 | 18.8 | 27.68 | 17.3 | 17.3 | 16.85 | 16.85 |
| Dry film thickness [µm] | 53.93 | 46.87 | 42.47 | 40.87 | 51.6 | 71.27 | 105.5 | 140.3 | 108.0 | 123.4 |
| Residual moisture [%] | 10.41 | 9.89 | 10.33 | 11.42 | 11.01 | 6.46 | 4.16 | 1.87 | 2.52 | 3.36 |
| Maximum tension stress [MPa] | 0.15 | 0.34 | 0.35 | 0.36 | 0.22 | 0.10 | 0.43 | 0.35 | 0.59 | 0.64 |

## 3. Evaluation

The coated and laser dried anodes are analyzed regarding different quality characteristics. In the course of the analysis the residual moisture, adhesion force, surface quality and dry film thickness were measured. In the following, the results of the process related analysis of the anode quality are presented and the presumed cause-effect relationships are explained.

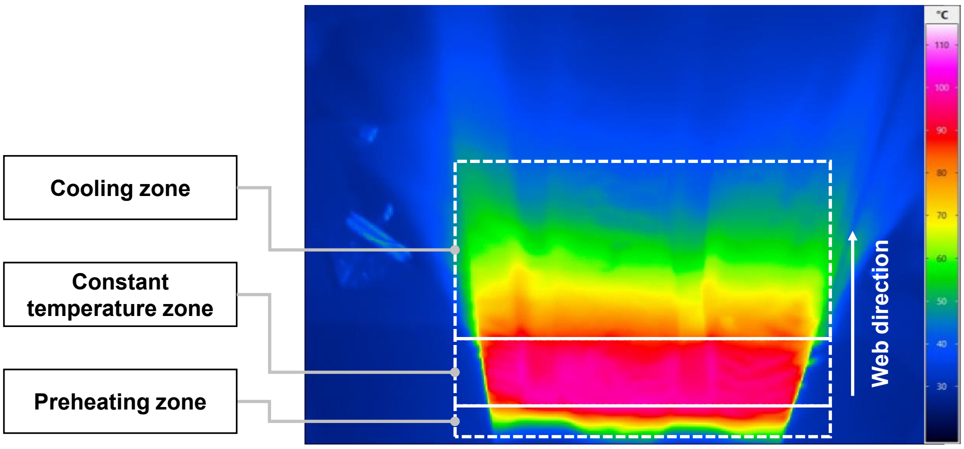


Figure 7: Thermographic analysis of the VCSE laser drying process

The thermographic analysis in Figure 7 shows that the VCSE laser drying process can be divided into 3 zones. The first zone represents the preheating zone. Due to the typically very low diffusion range of VCSEL arrays, this zone appears to be very short when using this technology without the addition of diffusor optics. The preheating zone is followed by the constant temperature zone. In this area, where most of the solvents are removed, the laser intensity must be specifically adapted to the evaporation of the solvent contained in the slurry. The third zone represents the cooling zone. In addition to convection air flows, cooling in this zone can be enhanced by contact with the resistance plate shown in Figure 4.

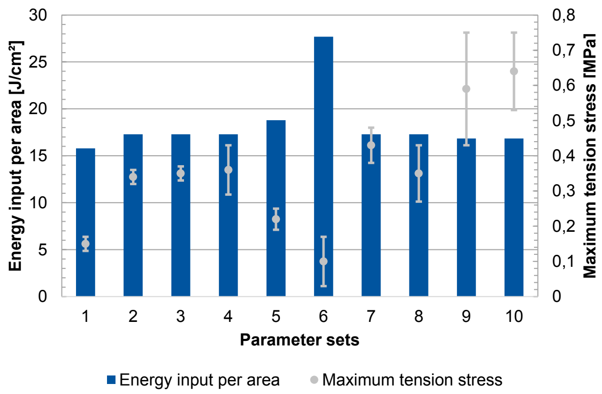


Figure 8: Energy input and tension stress

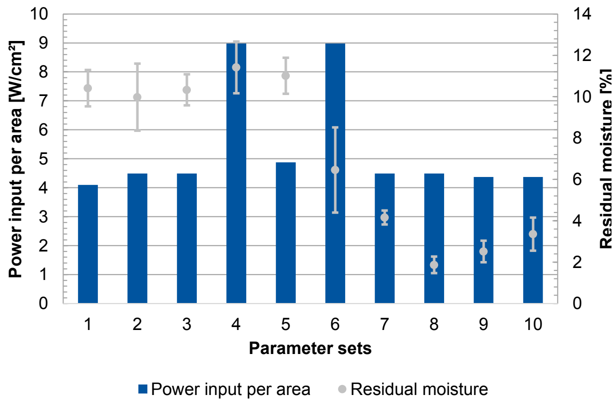


Figure 9: Power input and residual moisture

While Figure 8 shows the energy input per area over the maximum tensile stress, Figure 9 shows the power input per area over the measured residual moisture content. The analyzed experiments refer to the parameter sets described in Table 2 as well as the slurry mixtures shown in Table 1. With respect to the energy input per area, the parameters sets 3 and 4 show identical values of 17.3 J/cm². However, if the values of Figure 9 are taken into account, it can be seen that the power input per area has doubled from parameter set 3 to 4. The reason for this is that the web speed was increased from parameter set 3 to 4 from 0.8 to 1.6 m/min. To compensate for the increased web speed, the number of activated heating zones was increased from 18 to 36. Hereby the heating zones of parameter set 3 were switched off intermittently, as shown in the right sided example in Figure 6. The activation of the heating zones of all other parameter sets, including parameter set 4, were carried out according to the left sided example in Figure 6.

Within the test series, parameter set 6 experienced the highest energy input per area with 27.68 J/cm². To achieve this energy input, 36 heating zones were activated with a laser output power of 11.5%. At the same time, it is noticeable that parameter set 6 has the lowest adhesion values in the test series. Reasons for the poor adhesion values are most likely due to the effect of »binder migration« within the wet film layer. In this case, the rapid evaporation of the solvent leads to an accumulation of the binder material near the surface area [23]. According to JAISER et al. the inhomogeneous distribution of the binders also minimizes the adhesion forces between the copper foil and the active material [24].

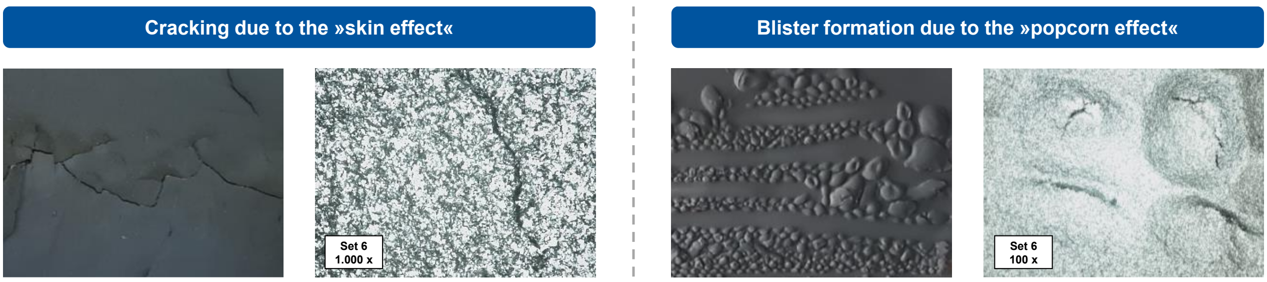


Figure 10: Microscopic images of defects in the dried coating of parameter set 6

Furthermore, the low adhesion values can be explained by an approximation or even exceeding of the decomposition temperature of the CMC and SBR components. The thermal stress within parameter set 6 leads also to the formation of cracks and blisters, which are shown in Figure 10. This represents a further explanation for the low adhesion results of the 6th parameter set. The formation of cracks on the electrode surface can be partially attributed to the »skin effect«. Within this effect, an excessively high power input per area in combination with a high drying rate causes the solvent to evaporate too quickly from the boundary layers. As a result, the outer layer of the active material is dried and forms a consolidated skin that reduces the penetrability of solvents. After the formation of this consolidation layer, solvent is still present in the deeper levels of the coating layer. This residual solvent is further heated by the absorbed laser radiation, which causes an expansion whereby the solvent can only slowly escape due to the limited permeability of the consolidation layer. Moreover, the rise of solvent by means of capillary forces is also reduced by this effect. This results in a pressure increase below the consolidation layer, so that the consolidation layer bulges outwards and blisters as well as cracks are formed. Through these cracks, the solvent is able to evaporate from the active material layer. According to KUMBERG et al. the application of higher layer thicknesses also results in a higher probability of cracking [25]. A further increase in the power input can also result in a »popcorn effect«. This is manifested in an explosion-like expansion of the contained solvent as a result of a far too high power input. The principles of the skin effect and the popcorn effect are roughly illustrated in Figure 11.

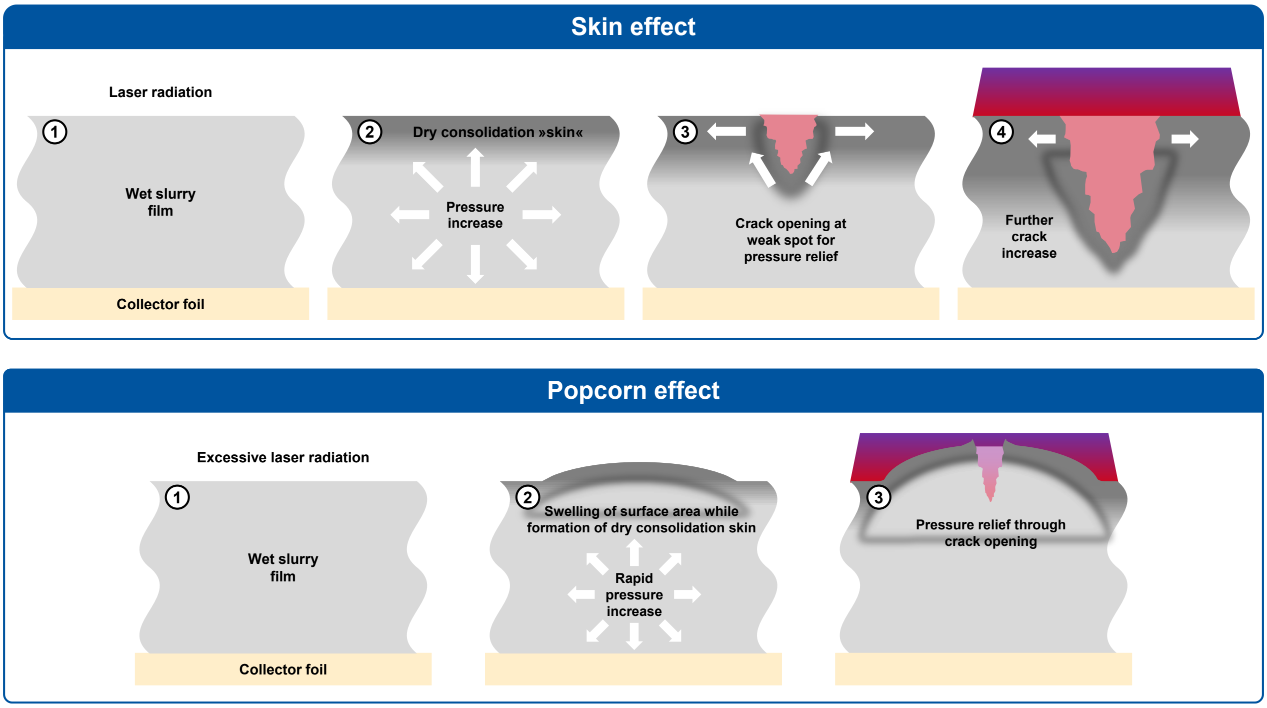


Figure 11: Illustration of the »skin effect« and »popcorn effect«

Figure 8 also shows that the parameter sets 9 and 10 have the highest average tensile values of 0.59 and 0.64 MPa. At the same time, both parameters have set humidity values of less than 3.5%. It is important to note that the parameter sets 9 and 10 with 108.0 and 123.4 µm show higher dry film thicknesses with lower solvent content of 38.4 wt.% compared to some of the other parameter sets. Despite the experimental pilot setup, these values are not far from electrodes produced in some series production. This highlights the applicability of the laser drying method for the production of electrodes and can be seen as a proof of concept for the use of the VCSEL technology.

## 4. Conclusion

Vertical-cavity surface-emitting laser (VCSEL) represent an innovative technology for energy-efficient and throughput increased electrode drying. Other research studies have shown that drying times could be reduced by up to 80% as well as energy consumption could be decreased by more than 50% using similar laser drying technologies [15, 20].

In this experimental study, the drying of several slurry formulations for anodes under different parameter settings was investigated using the VCSE laser technology. For this purpose, the experimental setup as well as the general structure of VCSE laser drying modules was described. Due to their high power density combined with high compactness, new types of machine setups can also be realized. The VCSEL technology, for example, enables the vertical coating and drying of electrodes, which was also investigated in this study.

In pilot operation at web speeds of up to 1.6 m/min, it was shown that residual moisture and adhesion values close to those of mass-produced electrodes could be generated. Thereby, the obtained research results can be considered as a proof of concept for the applicability of VCSE lasers for drying electrodes.

Due to the tremendously large number of different influencing variables, including numerous process and material parameters, the appropriate implementation of the VCSEL technology represents a complex challenge. The main target for the successful integration of the laser drying process is to achieve uniform drying, while avoiding phenomena such as »binder migration«, »skin effect« or even the »popcorn effect« in the event of excessively high energy input. The further increase of the web speeds as well as the investigation of the VCSEL application in hybrid drying processes to utilize synergies between different drying technologies represent further objectives for future research.

Further advantages of the VCSEL technology lie in its high control dynamics. For example, this is shown by the possibility of location-selected energy input, its precisely controlled energy transmission or its fast switch-on and switch-off times. The integration of sensor technology as well as the development of intelligent control and machine learning algorithms represent further open research topics with regard to VCSE laser drying. Lastly, it is also important to investigate the coating material more closely with the aim of developing laser-optimized material systems. In summary, VCSE laser drying represents a promising technology for energy efficient and quality-optimized lithium-ion battery production. Additionally, this technology bears great potential to significantly reduce greenhouse gas emissions during the manufacturing of battery cells.

**Acknowledgements**

This work is part of the Project LaserScale. The project has received funding from the German Federal Ministry of Education and Research (BMBF) under the funding code 03XP0316A. The authors are responsible for the content of this publication.

## References

[1] Korthauer, R. (Ed.), 2019. Lithium-ion batteries: Basics and applications.

[2] Susarla, N., Ahmed, S., Dees, D., 2018. Modeling and analysis of solvent removal during Li-ion battery electrode drying. Journal of Power Sources 378, 660–670.

[3] Schulze, O. (Ed.), 2022. Elektromobilität - ein Ratgeber für Entscheider, Errichter, Betreiber und Nutzer: Facetten zu Ladeinfrastruktur, Subventionsregeln, Kosten und Handling. Springer, Wiesbaden, Heidelberg, 307 pp.

[4] Betz, J., Buchert, M., Dolega, P., Bulach, W., 2021. Resource consumption of the passenger vehicle sector in Germany until 2035–the impact of different drive systems: Study on behalf of the German Federal Ministry for the Environment, Nature Conservation and Nuclear Safety.

[5] Clausen, J., Grimm, A., Pfaff, M., 2022. Die erfolgreiche Transformation der Automobilbranche.

[6] Kampker, A., Vallée, D., Schnettler, A., 2018. Elektromobilität. Springer Berlin Heidelberg, Berlin, Heidelberg, 416 pp.

[7] Neef, C. (Ed.) 2022. Development perspectives for lithium-ion battery cell formats, Fraunhofer ISI.

[8] Heimes, H., Kampker, A., Lienemann, C., Locke, M., Offermanns, C., Michaelis, S., Rahimzei, E., 2018. Lithium-ion battery cell production process. PEM der RWTH Aachen University.

[9] Küpper, D., Kuhlmann, K., Wolf, S., Pieper, C., Xu, G., Ahmad, J., 2018. The Future of Battery Production for Electric Vehicles. BCG Global.

[10] Degen, F., Schütte, M., 2022. Life cycle assessment of the energy consumption and GHG emissions of state-of-the-art automotive battery cell production. Journal of Cleaner Production 330, 129798.

[11] Liu, Y., Zhang, R., Wang, J., Wang, Y., 2021. Current and future lithium-ion battery manufacturing. iScience 24 (4), 102332.

[12] von Horstig, M., Schoo, A., Loellhoeffel, T., Mayer, J.K., Kwade, A., 2022. A Perspective on Innovative Drying Methods for Energy-Efficient Solvent-Based Production of Lithium-Ion Battery Electrodes. Energy Tech, 2200689.

[13] Bryntesen, S., Strømman, A., Tolstorebrov, I., Shearing, P., Lamb, J., Stokke Burheim, O., 2021. Opportunities for the State-of-the-Art Production of LIB Electrodes - A Review. Energies 14 (5), 1406.

[14] Moench, H., Deppe, C., Dumoulin, R., Gronenborn, S., Gu, X., Heusler, G., Miller, M., Pekarski, P., Pruijmboom, A., 2012. Modular VCSEL solution for uniform line illumination in the kW range, in: High-Power Diode Laser Technology and Applications X. SPIE LASE, San Francisco, California, USA. Saturday 21 January 2012. SPIE, 82410B.

[15] Vedder, C., Hawelka, D., Wolter, M., Leiva, D., Stollenwerk, J., Wissenbach, K., 2016. Laser-based drying of battery electrode layers, in: International Congress on Applications of Lasers & Electro-Optics. ICALEO 2016: 35th International Congress on Applications of Lasers & Electro-Optics, San Diego, California, USA. October 16–20, 2016. Laser Institute of America, N501.

[16] Pfleging, W., 2018. A review of laser electrode processing for development and manufacturing of lithium-ion batteries. Nanophotonics 7 (3), 549–573.

[17] Wolf, S., Neb, D., Hölting, F., Özkan, B., Clever, H., Dorn, B., Heimes, H., Kampker, A. 2023. Laser Drying Of Graphite Anodes For The Production Of Lithium-Ion Batteries - A Process- And Material-Side Analysis For Sustainable Battery Production.

[18] Neb, D., Stanislav, K., Clever, H., Dorn, B., Kampker, K. 2022. Current advances on laser drying of electrodes for lithium-ion battery cells.

[19] Propawe, R. (Ed.), 2005. Lasertechnik für die Fertigung: Grundlagen, Perspektiven und Beispiele für den innovativen Ingenieur. Springer Berlin Heidelberg, Berlin, Heidelberg, 526 pp.

[20] Wolf, S., Garbade, L., Göken, V., Tien, R., Börner, M., Neb, D., Heimes, H., 2023. Process and Material Analysis of Laser- and Convection-Dried Silicon - Graphite Anodes for Lithium-Ion Batteries. WEVJ 14 (4), 87.

[21] Gronenborn, S., Miller, M., Heusler, G., Mönch, H., 2012. Optical components and optical systems for VCSEL diode laser systems. Advanced Optical Technologies 1 (5).

[22] Pruijmboom, A., Apetz, R., Conrads, R., Deppe, C., Derra, G., Gronenborn, S., Gu, X., Kolb, J.S., Miller, M., Moench, H., Ogiewa, F., Pekarski, P., Pollmann-Retsch, J., Weichmann, U., 2015. VCSEL arrays expanding the range of high-power laser systems and applications, in: International Congress on Applications of Lasers & Electro-Optics. ICALEO 2015: 34th International Congress on Laser Materials Processing, Laser Microprocessing and Nanomanufacturing, Atlanta, Georgia, USA. October 18–22, 2015. Laser Institute of America, pp. 1–8.

[23] Font, F., Protas, B., Richardson, G., Foster, J.M., 2018. Binder migration during drying of lithium-ion battery electrodes: Modelling and comparison to experiment. Journal of Power Sources 393, 177–185.

[24] Jaiser, S., Müller, M., Baunach, M., Bauer, W., Scharfer, P., Schabel, W., 2016. Investigation of film solidification and binder migration during drying of Li-Ion battery anodes. Journal of Power Sources 318, 210–219.

[25] Kumberg, J., Müller, M., Diehm, R., Spiegel, S., Wachsmann, C., Bauer, W., Scharfer, P., Schabel, W., 2019. Drying of Lithium-Ion Battery Anodes for Use in High-Energy Cells: Influence of Electrode Thickness on Drying Time, Adhesion, and Crack Formation. Energy Technol. 7 (11), 1900722.

**Biography**

**Daniel Neb** (*1992) is the group lead of the department “Battery Production Management” (BPM) at PEM of RWTH Aachen University, where he also studied Mechanical Engineering with a specialization in Automotive Engineering.

**Sebastian Wolf** (*1997) is research associate in the group “Battery Production Management” (BPM) at the Chair of Production Engineering of E-Mobility Components (PEM) at RWTH Aachen University, where he also studied Mechanical Engineering and Business Administration.

**Benedict Ingendoh** (*1998) is research associate in the group “Battery Production Technology” (BPT) at the Chair of Production Engineering of E-Mobility Components (PEM) at RWTH Aachen University, where he also studied Mechanical Engineering and Business Administration.

**Simon Klein** (*1999) is student assistant at PEM of RWTH Aachen University, where he also studies Mechanical Engineering with a specialization in Automotive Engineering.

**Benjamin Dorn** (*1990) is chief engineer for Production Technology and Organization at PEM of RWTH Aachen University. He studied Mechanical Engineering and Business Administration there.

**Heiner Hans Heimes** (*1983) was PEM’s executive chief engineer from 2019 to 2023. In March 2023, he was appointed associate professor with a focus on "Production Engineering for Lithum-Ion Batteries". Together with Professor Achim Kampker, he is responsible for the strategic and operational management of the PEM Chair.

**Achim Kampker** (*1976) is head of PEM at RWTH Aachen. He also acts as member of the executive board of the Fraunhofer FFB in Münster. Achim Kampker is involved in various expert groups of the federal and state governments.